Decreased fibrogenesis after treatment with pirfenidone in a newly developed mouse model of intestinal fibrosis

Meier, Remo ; Lutz, Christian ; Cosín-Roger, Jesus ; Fagagnini, Stefania ; Bollmann, Gabi ; Hünerwadel, Anouk ; Mamie, Celine ; Lang, Silvia ; Tchouboukov, Alexander ; Weber, Franz E ; Weber, Achim ; Rogler, Gerhard ; Hausmann, Martin

Abstract: BACKGROUND Fibrosis as a common problem in patients with Crohn's disease is a result of an imbalance toward excessive tissue repair. At present, there is no specific treatment option. Pirfenidone is approved for the treatment of idiopathic pulmonary fibrosis with both antifibrotic and anti-inflammatory effects. We subsequently investigated the impact of pirfenidone treatment on development of fibrosis in a new mouse model of intestinal fibrosis. METHODS Small bowel resections from donor mice were transplanted subcutaneously into the neck of recipients. Animals received either pirfenidone (100 mg/kg, three times daily, orally) or vehicle. RESULTS After administration of pirfenidone, a significantly decreased collagen layer thickness was revealed as compared to vehicle (9.7 ± 1.0 versus 13.5 ± 1.5 µm, respectively, **P < 0.001). Transforming growth factor- and matrix metalloproteinase-9 were significantly decreased after treatment with pirfenidone as confirmed by real-time PCR (0.42 ± 0.13 versus 1.00 ± 0.21 and 0.46 ± 0.24 versus 1.00 ± 0.62 mRNA expression level relative to GAPDH, respectively, *P < 0.05). Significantly decreased transforming growth factor- after administration of pirfenidone was confirmed by Western blotting. CONCLUSION In our mouse model, intestinal fibrosis can be reliably induced and is developed within 7 days. Pirfenidone partially prevented the development of fibrosis, making it a potential treatment option against Crohn's disease-associated fibrosis.

DOI: https://doi.org/10.1097/MIB.0000000000000716

Decreased Fibrogenesis After Treatment with Pirfenidone in a Newly Developed Mouse Model of Intestinal Fibrosis

Remo Meier, Christian Lutz,* Jesus Cosín-Roger, MD,*,† Stefania Fagagnini, MD,* Gabi Bollmann,* Anouk Hünerwadel,* Celine Mamie,* Silvia Lang,* Alexander Tchouboukov, PhD,‡ Franz E. Weber, MD,‡ Achim Weber, MD, PhD,§ Gerhard Rogler, MD, PhD,* and Martin Hausmann, PhD**

Background: Fibrosis as a common problem in patients with Crohn's disease is a result of an imbalance toward excessive tissue repair. At present, there is no specific treatment option. Pirfenidone is approved for the treatment of idiopathic pulmonary fibrosis with both antifibrotic and anti-inflammatory effects. We subsequently investigated the impact of pirfenidone treatment on development of fibrosis in a new mouse model of intestinal fibrosis.

Methods: Small bowel resections from donor mice were transplanted subcutaneously into the neck of recipients. Animals received either pirfenidone (100 mg/kg, three times daily, orally) or vehicle.

Results: After administration of pirfenidone, a significantly decreased collagen layer thickness was revealed as compared to vehicle (9.7 ± 1.0 versus 13.5 ± 1.5 μm, respectively, $^{**}P < 0.001$). Transforming growth factor–β and matrix metalloproteinase–9 were significantly decreased after treatment with pirfenidone as confirmed by real-time PCR (0.42 ± 0.13 versus 1.00 ± 0.21 and 0.46 ± 0.24 versus 1.00 ± 0.62 mRNA expression level relative to GAPDH, respectively, $^{*}P < 0.05$). Significantly decreased transforming growth factor–β after administration of pirfenidone was confirmed by Western blotting.

Conclusion: In our mouse model, intestinal fibrosis can be reliably induced and is developed within 7 days. Pirfenidone partially prevented the development of fibrosis, making it a potential treatment option against Crohn's disease–associated fibrosis.

(Inflamm Bowel Dis 2016;22:569–582)

Key Words: fibrogenesis, fibrosis, intestinal, pirfenidone, treatment, transplantation, graft, mouse model, TGF-β, MMP-9

Severe and persistent mucosal tissue damage is a main feature of inflammatory bowel disease (IBD). Tissue injury triggers an important inflammatory response, which in turn leads to the initiation of a reparatory process.[1–3] Rapid and adequate healing is essential to reduce the exposure of the underlying tissue to luminal antigens and potential pathogens and to restore a tight barrier. Furthermore, adequate wound healing physiologically is the result of an exquisite balance between multiple profibrotic and antifibrotic stimuli on extracellular matrix–producing cells.[4–7] The primary cellular mediator of fibrosis is the myofibroblast, which can be generated from several sources.[8] Excessive tissue repair promotes fibrosis and impairs gastrointestinal function and is a common clinical problem in patients with Crohn's disease (CD).

Fibrosis is increasingly being recognized as an important cause of morbidity and mortality in many chronic inflammatory diseases. The pathogenesis of fibrosis in patients with CD, however, is still poorly understood. Intestinal fibrosis leads to stricture formation in 30% to 50% of patients with CD[9,10] and requires surgery in approximately 80% of strictured patients.[9]

Administration of potent anti-inflammatory agents effectively treats inflammatory flares but may not alter the course of intestinal fibrosis and fail to prevent the formation of strictures.[11,12] Despite earlier initiation of immunosuppressants or biologicals during the course of CD, the percentage of patients requiring intestinal surgery due to the occurrence of stricturing complications has only decreased slightly.[13] Recently, it was demonstrated that treating inflammation may not be sufficient to prevent the progression of fibrosis. Furthermore, there is evidence that intestinal fibrogenesis after being once initiated is—at least to some extent—a self-perpetuating process.[14] Therefore, many experts point to the unmet clinical need of a medical treatment to prevent or inhibit fibrogenesis/fibrosis.

Supplemental digital content is available for this article. Direct URL citations appear in the printed text and are provided in the HTML and PDF versions of this article on the journal's Web site (www.ibdjournal.org).

Received for publication October 20, 2015; Accepted December 14, 2015.

From the *Clinic of Gastroenterology and Hepatology, Department of Internal Medicine, University Hospital Zurich, Zurich, Switzerland; †Departamento de Farmacología and CIBERehd, Facultad de Medicina, Universidad de Valencia, Valencia, Spain; ‡Division of Cranio-Maxillofacial and Oral Surgery, Center for Dental Medicine, Oral Biotechnology & Bioengineering, University of Zurich, Zurich, Switzerland; and §Institute of Surgical Pathology, University Hospital Zurich, Zurich, Switzerland.

G. Rogler discloses grant support from AbbVie, Ardeypharm, MSD, FALK, Flamentera, Novartis, Roche, Tillots, UCB, and Zeller. The remaining authors have no conflicts of interest to disclose.

Reprints: Martin Hausmann, PhD, Division of Gastroenterology and Hepatology, University Hospital Zürich, University of Zurich, 8091 Zurich, CH-Switzerland (e-mail: martin.hausmann@usz.ch).

DOI 10.1097/MIB.0000000000000716

Published online 5 February 2016.

The clinical investigation of intestinal fibrosis is confined to the limited amount of biological material available from patients. Establishing an animal model that reflects the development of intestinal fibrosis in humans is therefore regarded to be a prerequisite for the development of drugs targeted at intestinal fibrosis. To develop such an animal model, we adopted a rat airway transplant model of bronchiolitis obliterans.[15] Recently, we described a new model of intestinal fibrosis by performing a heterotopic transplantation of small bowel resections in rats. The loss of intestinal epithelial morphology, exaggerated collagen deposition, expression of profibrotic mediators, and progressive luminal wall thickening culminating in a veritable fibrotic occlusion of the intestinal lumen faithfully reflect the histologic and molecular features of human intestinal fibrosis. The simplicity and efficiency of this model may greatly aid the study of the pathogenesis of intestinal fibrosis and the development of suitable therapeutics to prevent and treat intestinal fibrosis[16]. However, to allow the study of mechanistic aspects of intestinal fibrosis in knock-out animals and to allow drug treatment experiments with lower amounts of substance, the model had to be transferred into mice.

In this study, we describe the successful establishment of a mouse model of intestinal fibrosis in which we investigated pirfenidone as a possible candidate for an antifibrotic treatment in intestinal fibrosis.

Pirfenidone (Esbriet; Hoffmann-La Roche AG, Basel, Switzerland) is an orally bioavailable small molecule developed by InterMune Inc. (Brisbane, CA). It exhibits well-documented antifibrotic and anti-inflammatory properties in a variety of animal and in vitro models in different organs, including fibrosis of the lung,[17] kidneys,[18] heart,[19] liver,[20] and skin.[21] The exact molecular mechanism of action so far is unknown.[22] Pirfenidone influences significantly the production of various cytokines and growth factors, with the most commonly reported effect being a reduction of transforming growth factor–β (TGF-β).[19,20,23] Others reported decreased interleukin (IL)-1β, IL-6, and monocyte chemotactic protein (MCP)-1 protein after treatment with pirfenidone shown in supernatants of lung homogenates in the bleomycin-induced murine model of pulmonary fibrosis.[23] Decreased transcript levels of the matrix metalloproteinase (MMP)-2 and tissue inhibitor of metalloproteinase (TIMP)-1 after treatment with pirfenidone were shown in a dimethylnitrosamine-induced rat model of liver fibrosis.[20] Decreased transcript levels of collagens I and III after treatment with pirfenidone were shown in primary cultures of human myometrial and leiomyoma smooth muscle cells.[24]

A meta-analysis of progression-free survival time in three phase III clinical trials of pirfenidone in patients with idiopathic pulmonary fibrosis (IPF) reported a significant overall treatment benefit.[25] It was approved in Japan as Pirespa in 2008. It was approved in China and in Europe for the treatment of IPF in 2011 and in October 2014 in the United States by the Food and Drug Administration.

In this study, we describe our rapid and reliable animal model of intestinal fibrosis and show that pirfenidone also prevents intestinal fibrosis, indicating its potential as treatment option for stricturing CD.

MATERIALS AND METHODS

Animals

Female B6-Tg (UBC-GFP) 30Scha/J donor mice (GFP-Tg) weighing 20g were bred locally. C57BL/6J-Crl1 mice (C57BL/6) were obtained from Charles River. BALB/c mice (BALB/c) were obtained from Jackson Laboratories. The animals received standard laboratory mouse food and water ad libitum. They were housed under specific pathogen-free conditions in individually ventilated cages. The experimental protocol was approved by the local Animal Care Committee of the University of Zurich (registration number: ZH183/2014).

Heterotopic Intestinal Transplant Model

The heterotopic mouse intestinal transplant model is an adaption of the heterotopic transplantation model of intestinal fibrosis in rats, which has been previously described in detail.[16] In short, donor small bowel resections were extracted and transplanted subcutaneously into the neck of recipient animals. Transplantation was performed between mice of the same gender. All procedures were performed using a sterile nontouch technique. Donor mice were killed by neck dislocation. After an initial anterior midline incision, the abdomen was opened completely to avoid contamination of the inner organs with hair. The small bowel was then exposed and carefully unfolded by cutting mesentery where necessary. From the small bowel proximal to the cecum, a segment of 6 cm was excised. The resection was then flushed with 5 mL of 0.9% NaCl to remove stool and divided into 6 equal 10-mm parts. Resections were kept moist with 0.9% NaCl solution, whereas the recipient animals were prepared for transplantation (see Fig. A, Supplemental Digital Content 1, http://links.lww.com/IBD/B209). Recipient animals were anesthetized with isoflurane, and ocular lubricant was applied (Vitamine A Blache Augensalbe 5g #109778). A small area of the back was shaved to avoid contamination with hair. Two subcutaneous pouches were prepared through a small incision perpendicular to the body axis on either side of the neck (Fig. B, Supplemental Digital Content 1, http://links.lww.com/IBD/B209). A small bowel resection was implanted into each of the subcutaneous pockets (Fig. C, Supplemental Digital Content 1, http://links.lww.com/IBD/B209), and the skin was closed using vicryl 5-0 stitches or a 3M Precise Vista Skin Stapler (Fig. D, Supplemental Digital Content 1, http://links.lww.com/IBD/B209). A single dose of cefazolin (Kefzol, Teva Pharma AG, Basel, Switzerland; 1g diluted in 2.5-mL aqua dest) was applied intraperitoneally as infection prophylaxis. The time interval between graft resection and subsequent implantation was less than 15 minutes. No anesthesia-related recipient death, posttransplantation recipient death, or evidence of infection was observed in any of the animals.

Recipient mice were killed by neck dislocation. Intestinal grafts were explanted up to 21 days after transplantation. Numerous blood vessels stretched toward the transplanted tissue (see Fig. H, Supplemental Digital Content 1, http://links.lww.com/IBD/B209) where they formed a dense network (see Fig. I, Supplemental Digital Content 1, http://links.lww.com/IBD/B209). At

explantation, each graft was divided into 3 equal segments. One segment was fixed in 4% formalin and prepared for histopathological assessment. The other segments were snap frozen in liquid nitrogen and stored at −80°C until RNA extraction or lysis in MPER buffer.

Pirfenidone Preparation and Application

Esbriet tablets (276 mg, InterMune Inc., now part of the F. Hoffmann-La Roche AG) were dissolved in 14-mL sterile water to a pirfenidone concentration of 20 mg/mL. Pirfenidone was orally administered to recipient mice by oral gavage using a gastric tube. Pirfenidone (100 μL = 100 mg/kg) was administered 3 times a day orally (7:00–10:00, 13:00–16:00, 19:00–22:00) for 6 days after transplantation. Sterile water was used as vehicle control. For in vitro experiments, Pirfenidone was dissolved in methanol.

Stent Insertion

A cobalt chromium coronary stent coated with epoxy resin (Invatec Skylor, Roncadelle, Italy) measuring 10 mm in length and 2 mm in diameter was used. After isolating a section of intestine from a C57BL/6 donor mouse, a stent was inserted into the open lumen of the resection before then being implanted in the subcutaneous neck pouch of a B6 recipient mouse. The graft was explanted at day 7 and embedded in epoxy resin for histological analysis.

Paragon and Giemsa Staining

The specimens were prepared with a sequential water substitution process, then placed in xylene for 72 hours, and infiltrated by placing them in methyl methacrylate (MMA) for 72 hours (Fluka 64,200) followed by 3 days in 100-mL MMA + 2-g dibenzoylperoxid (Fluka 38,581) at 4 C°. Samples were embedded by placing them in 100-mL MMA + 3-g dibenzoylperoxid + 10-mL plastoid N or dibutyl phthalate (Merck 800 19.25) and allowing polymerization to occur at 37 C° in an incubator. After embedding, the specimens were sectioned by a diamond band saw (Exakt 300P) glued to a support and sectioned again, so that a 200-μm thick sample from the middle was attached to the support. The thickness of this sample was further reduced to 40 to 60 μm by a grinding machine (Exakt 420 CS). To visualize tissues, the samples were Paragon and Giemsa stained. Digital images were taken and processed with an image program (Adobes Photoshop CS3).

Immunohistochemistry

TGF-β1 was stained with a rabbit polyclonal antibody from Santa Cruz Biotechnology Inc. (Dallas, TX) (#sc-146, dilution 1:200, immunostainer Leica Bond III Stainer, pretreatment: Bond Epitope Retrieval Buffer 2 for 20 minutes, detections kit: Bond Polymer Refine Detections Kit, all reagents from Bond Leica). The sections were examined with the Imager Z2 microscope (Carl Zeiss AG, Oberkochen, Germany) and the software AxioVision (Zeiss). Sirius red–stained slides were analyzed in bright field using a polarization filter. Under polarized light, sirius red–stained collagen assumes a palette of colors ranging from green to red as a sign for fibrotic process maturation. Collagen layer thickness was determined by an investigator blinded to experiment. Thickness was calculated from at least 8 places in representative areas at 10-fold magnification.

TaqMan Gene Expression Assays

α-SMA Mm00725412_s1, BCL-$_{XL}$ Mm00437783_m1, MMP-9 Mm00442991_m1, MMP-2 Mm00439498_m1, TIMP-1 Mm00441818_m1, TGF-β1 Mm01178820_m1, lysyl oxidase–like 2 (LOXL-2) Mm00804740_m1, collagen type I alpha 1 (Col1a1) Mm00801666_g1, collagen type III alpha 1 (Col3a1) Mm01254476_m1, and GAPDH 4352339E. The relative cDNA concentration for the gene of interest was calculated using the ddCt method.

Cell Viability Assay

Primary murine colonic fibroblasts were isolated as described earlier.[26] Five thousand colonic fibroblasts per well were grown in triplicate cultures in 96 well plates. The final volume of culture medium in each well was 100 μL. Cells were starved 24 hours before stimulation. Cells were stimulated with 2 ng/mL TGF-β and 0-, 0.1-, 0.5-, and 1-mg/ml pirfenidone for 24 hours. The colorimetric assay (WST-8–based; Dojindo Molecular Technologies, Rockville, MD) for quantification of cell viability was performed according the manufacturer's protocol. Briefly, 10 μL cell counting kit (CCK)-8 solution was added to detect viable cells. The absorption was measured 4 hours after addition of the CCK-8 labeling at 450 nm using a microplate reader.

Wounding Assay

Colonic fibroblasts were seeded in culture inserts (#80209, width of cell-free gap, 500 μm ± 50 μm, ibidi). Confluent monolayers of cells were starved 24 hours before the wounding assay. The culture inserts were removed and cells were stimulated with 2-ng/mL TGF-β and 1-mg/ml pirfenidone. Wound closure was documented at t = 0, 24, and 48 hours with the Axiovert microscope (Zeiss) at 5-fold magnification and the Powershot camera (Canon, Tokyo, Japan).

Western Blot

Equal amounts of protein were loaded onto SDS/PAGE gels. Western blots were performed using monoclonal rabbit anti-mouse TGF-β (#3711S, Bioconcept, 1:1000), polyclonal rabbit anti-mouse β-actin (#4970, 13E5; Cell Signaling Technology, Cambridge, MA; 1:2000), and the horseradish peroxidase–conjugated secondary antibody goat anti-rabbit (#sc-2004; Santa Cruz, 1:2000), respectively. Focal adhesion kinase (FAK) protein detection was performed with specific antibodies to FAK (#3285; Cell Signaling, 1:1000) and phosphorylated tyrosine 397 of FAK (#3283; Cell Signaling, 1:1000), and incubation with peroxidase-conjugated secondary antibody goat anti-rabbit (#sc-2004; Santa Cruz, 1:2000). Luminescence of Western blots was quantified densitometrically with ImageJ.

Statistical Analysis

Statistical analysis for collagen layer thickness was performed using Kruskal–Wallis one-way analysis of variance on

ranks, all-pairwise multiple comparison procedures (Tukey test). Statistical analysis for qPCR was performed using Kruskal–Wallis one-way analysis of variance on ranks, all-pairwise multiple comparison procedures (Holm–Sidak method), or unpaired t-test when was appropriated. Differences were considered significant at a P value of < 0.05 (*) and highly significant at a P value of < 0.01 (**) and P value of < 0.001 (***).

Ethical Considerations

The experimental protocol was approved by the local Animal Care Committee of the University of Zurich (registration number: ZH183/2014).

RESULTS

Establishment of a Fast and Reliable Heterotopic Transplantation Model of Intestinal Fibrosis

To determine the relevance of the genetic background of donor and recipient in our heterotopic transplantation model of intestinal fibrosis, BALB/c mice were used as donors for allogeneic transplantation, whereas C57BL/6 were used as donors for isogeneic transplantation into C57BL/6 recipients. Eight isogeneic transplants (C57BL/6 into C57BL/6 mice) and 16 allogeneic transplants (BALB/c into C57BL/6 mice) were performed. Grafts were explanted up to 21 days after transplantation. Macroscopically, a reduction in the graft length appeared. Histologically evaluable tissue was recovered from all but 4 animals.

In EvG-stained histological cross sections, freshly isolated small intestine was characterized by an open lumen and distinctive epithelial crypts (Fig. 1A and C). At day 21 after transplantation, the lumen of intestinal grafts was obstructed by granulation tissue and fibrotic material (Fig. 1B and E). Intestinal grafts already had lost their typical crypt structure at day 2 after transplantation. At day 5 after transplantation, the loss of crypt structures was complete and a partial occlusion of the lumen was observed (Fig. 1D). At day 14, luminal occlusion was complete. Epithelial structure was lost in heterotopic intestinal of both isografts and allografts.

Collagen production and deposition in the intestinal transplants were determined by EvG staining in transmission light. The collagen layer thickness in harvested grafts was significantly increased after 7 and 21 days in a time-dependent manner ($P < 0.05$, Fig. 1F). To confirm the time-dependent increase in collagen and to differentiate between long-chain and short-chain collagen, we performed sirius red staining (see Fig. 2, Supplemental Digital Content 2, http://links.lww.com/IBD/B210). Freshly isolated intestinal samples showed mostly long-chained collagen (red stain) adjacent to the submucosa (see Fig. B, Supplemental Digital Content 2, http://links.lww.com/IBD/B210). The presence of short-chained collagen (yellow stain) increased continuously with time in the submucosa and in the luminal occlusion after transplantation (see Fig. D–N, Supplemental Digital Content 2, http://links.lww.com/IBD/B210). The loss of epithelial structure and luminal occlusion was observed irrespective of the genotype of donor and recipient mice.

As in the transplant model of bronchial fibrosis, the lumen of the transplanted bronchus/trachea does not collapse to the cartilage present, we investigated whether an open gut lumen would influence fibrosis in our intestinal transplant model. Subsequently, a coronary stent was inserted into a graft before transplantation in an attempt to preserve the gut lumen. C57BL/6 mice were used as both donor and recipient. After explantation at day 7, we observed a shortened graft and a pronounced infiltration of cells into the lumen, causing an almost complete occlusion (see Fig. 3, Supplemental Digital Content 3, http://links.lww.com/IBD/B211). Thus, the fibrotic model is effective irrespective of a preserved or collapsed lumen of the transplant.

Mediators of Fibrosis in the Heterotopic Transplant Model of Intestinal Fibrosis

To further substantiate that the observed changes represent fibrotic changes, expression of TGF-β was analyzed. Both BALB/c and C57BL/6 were used as donors for allogeneic and isogeneic transplantation. C57BL/6 mice were used as recipients. TGF-β was detected by immunohistochemistry along the crypt villus axis in mouse intestinal epithelial cells in freshly isolated intestinal samples (Fig. 2A, C and D). No TGF-β was detected in the *lamina propria*. Intense staining for TGF was found in the luminal occlusion in allografts from day 5 to day 21 (Fig. 2E, F). Intense staining for TGF was also found in heterotopic intestinal isografts (not shown).

Host Cells Infiltrate the Intestinal Graft

The presence of endogenous GFP in GFP-Tg recipient mice allowed for a genotype-specific staining to be performed. We could thus determine the origin of the lumen-obstructing cells. We performed isogeneic transplantation using C57BL/6 mice as donors and GFP-Tg mice as recipient. As expected, the freshly isolated intestinal resections from C57BL/6 mice are negative for GFP staining (Fig. 3A). An increase in infiltration of stained GFP cells ensued in a time-dependent manner. Initially, red-stained cells were visible exclusively in the submucosa and seemed to accumulate along the collagen layer (Fig. 3B). Subsequent time points showed progressive infiltration along the crypts and into the lumen (Fig. 3C–F). The collagen layer was free of red-stained cells.

Typical Fibrosis Mediators Are Decreased In Vitro in Colonic Fibroblasts After Treatment with Pirfenidone Treatment

We next investigated whether pirfenidone as an agent approved for the therapy and prevention of progress in IPF would be effective in vitro in colonic fibroblasts. TGF-β of 2 ng/mL significantly increased both MMP-9 and COL1A1 mRNA expression ($P < 0.05$ and $P < 0.01$, respectively, n = 2, see Fig. 4, Supplemental Digital Content 4, http://links.lww.com/IBD/B212) and was used for further stimulations. To determine effects of pirfenidone and TGF-β on the viability of colonic fibroblasts, we used a CCK-8

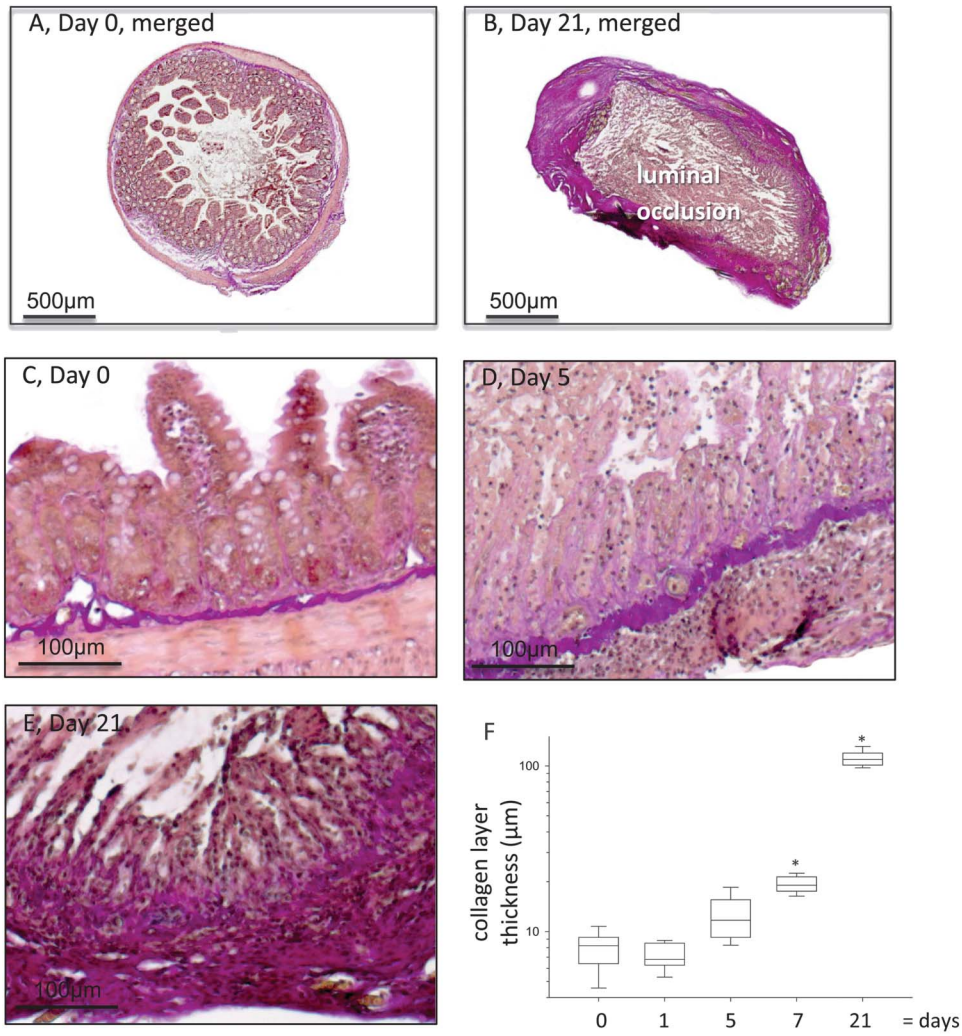

FIGURE 1. Increased collagen layer thickness in heterotopic intestinal grafts. Histologic cross sections of freshly isolated small intestine (A and C) and explanted at days 5 (D) and 21 (B and E) after transplantation. EvG staining of mouse small heterotopic intestinal grafts revealed an increase of collagen deposition in a time-dependent manner. (F) EvG staining revealed significantly increased collagen layer thickness (*$P < 0.05$, Kruskal–Wallis one-way analysis of variance on ranks, all-pairwise multiple comparison procedures (Tukey test), n = 9 for each column). BALB/c mice were used as donors for allogeneic transplantation; B6 were used as donors for isogeneic transplantation. B6 were used as recipients.

colorimetric assay for the quantification of cell viability (see Fig. 5, Supplemental Digital Content 5, http://links.lww.com/IBD/B213). Colonic fibroblasts showed an increase in cell viability after administration of pirfenidone in a dose-dependent manner (n = 5 each column). Cell viability was also significantly increased on TGF-β stimulation (162% ± 8%, n = 5) as compared with vehicle (set to 100%, n = 5, $P < 0.001$, see Fig. 5, Supplemental Digital Content 5, http://links.lww.com/IBD/B213) but did not further increase after treatment with additional pirfenidone.

In the absence of TGF-β stimulation, COL1A1 mRNA expression was significantly decreased in colonic fibroblasts after administration of 1-µg/mL pirfenidone (n = 5 each column, $P < 0.001$, Fig. 4A), and α-SMA mRNA expression was significantly decreased in a dose-dependent manner ($P < 0.05$; $P < 0.01$), whereas no changes in TGF-β expression were detected after treatment with pirfenidone. After additional TGF-β stimulation, a significantly decreased TGF-β, COL1A1, MMP-9, and α-SMA mRNA expression was detected after administration of pirfenidone in a dose-dependent manner compared with vehicle (n = 5 each column, $P < 0.01$, $P < 0.001$, Fig. 4A). In contrast, pro-survival BCL-$_{XL}$ mRNA expression was significantly increased after administration of 1-µg/mL pirfenidone independent of TGF-β stimulation (n = 5 each column, $P < 0.001$, Fig. 4A).

Tyrosine phosphorylation of p125 FAK is a central regulator of cell migration. Western blotting revealed unchanged expression of total FAK after treatment with pirfenidone (Fig. 4B, representative for 4 experiments). A quantification of FAK phosphorylation was also performed and revealed significantly increased pFAK after administration of pirfenidone in a dose-dependent manner independent of TGF-β stimulation

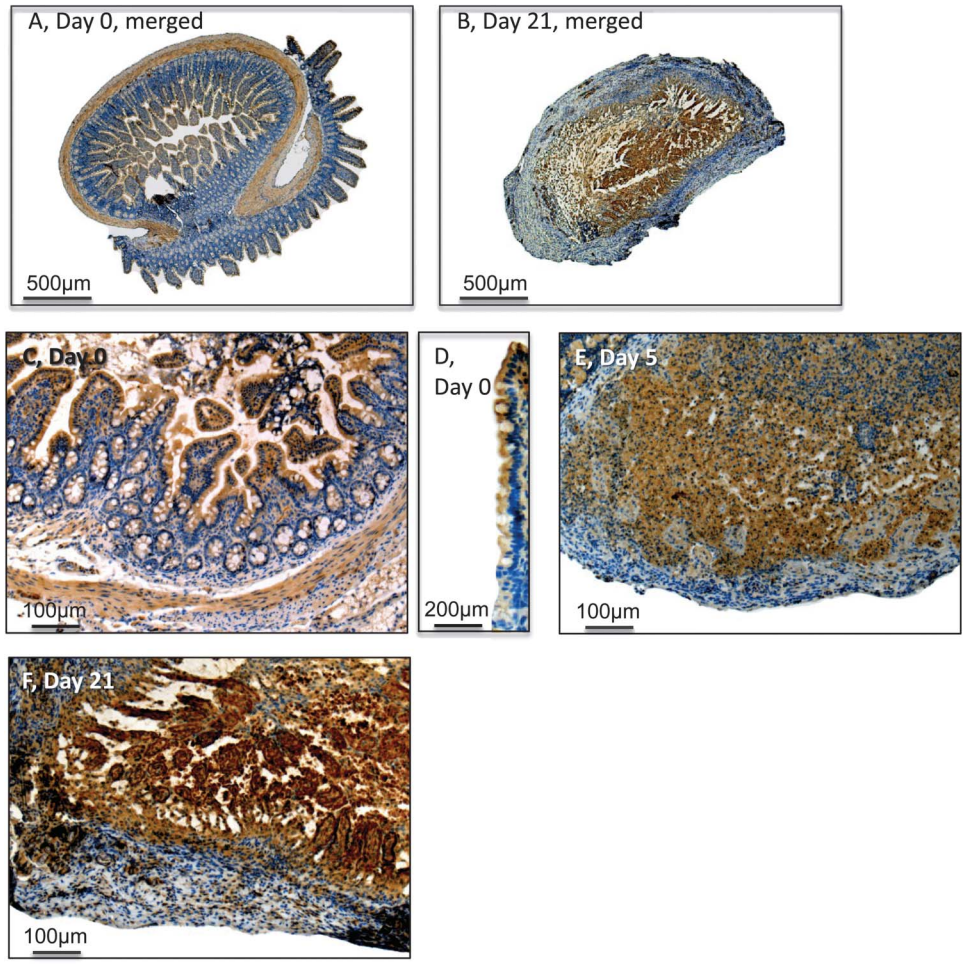

FIGUR E 2. Increased TGF-β in heterotopic intestinal grafts. Immunohistochemistry for TGF-β of mouse small intestine allografts. Histologic cross sections of freshly isolated small intestine (A, C, and D) and explanted at days 5 (E) and 21 (B and F) after transplantation. Transmitted light microscopy. In freshly isolated intestinal samples, TGF-β (brown) was increased along the crypt villus axis in mouse intestinal epithelial cells (D). Data revealed increased expression of TGF-β, a potent mediator of fibrosis. Each image is representative for 2 samples investigated. BALB/c mice were used as donors for allogeneic transplantation; B6 were used as donors for isogeneic transplantation. B6 were used as recipients.

(n = 4 each column, $P < 0.001$, Fig. 4B). Accordingly, gain of migratory potential of colonic fibroblasts could be confirmed in a wounding assay. In line with this, the wounding assay revealed an advanced wound closure after 24 and 48 hours after treatment with pirfenidone independent of TGF-β stimulation (see Fig. 6, Supplemental Digital Content 6, http://links.lww.com/IBD/B214, representative for 2 experiments).

Development of Intestinal Fibrosis Is Partially Prevented in Grafts After Administration of Pirfenidone

We next investigated whether pirfenidone would also be effective in our model of intestinal fibrosis. We performed isogeneic transplantation using GFP-Tg mice as donors and C57BL/6 mice as recipient. Body weight remained unchanged after treatment with pirfenidone (n = 7 mice) compared with vehicle (n = 8 mice, see Fig. 4, Supplemental Digital Content 4, http://links.lww.com/IBD/B212). Interestingly, a trend to lower body weight was seen after administration of pirfenidone, which may reflect dizziness triggered by pirfenidone as reported by others. We determined collagen production and deposition in the intestinal transplants by EvG staining in transmission light and under polarizing light (Fig. 5). The collagen layer thickness in harvested grafts from mice after treatment with pirfenidone was significantly decreased in comparison to the collagen layer thickness in grafts from vehicle treated mice ($P < 0.001$ for data obtained by transmission light and $P < 0.05$ for data obtained by polarized light microscopy, n = 12–14 grafts as indicated).

TGF-β1 Is Expression Significantly Decreased in Grafts After Administration of Pirfenidone

In the grafts, a significantly decreased TGF-β mRNA expression after pirfenidone treatment compared with vehicle

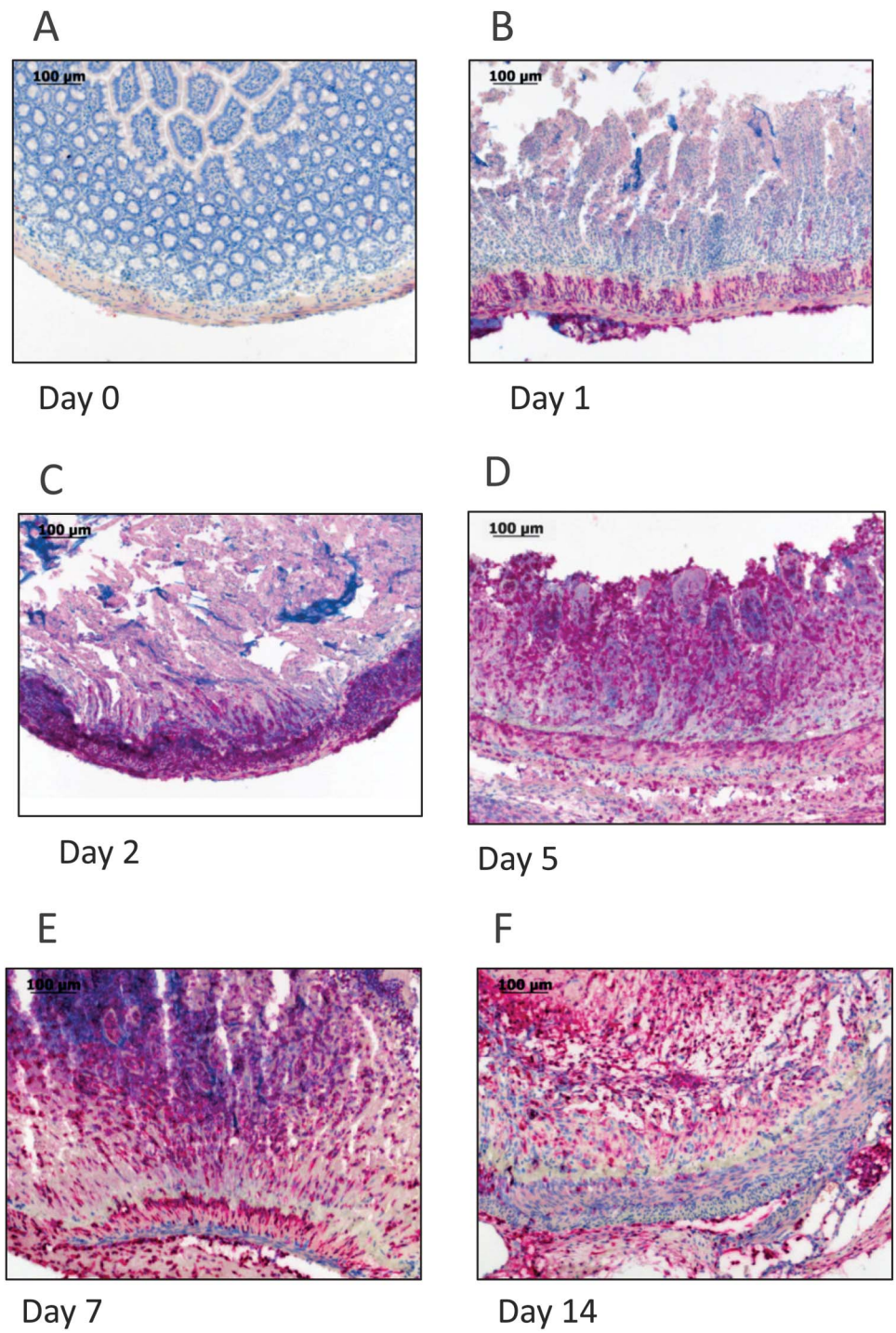

FIGURE 3. Host cells progressively infiltrate the intestinal graft. Immunohistochemistry of lumen-obstructing cells of recipient origin. Freshly isolated intestinal resections are negative for GFP (A). Increase in infiltration at days 1 (B), 2 (C), 5 (D), 7 (E), and 14 (F) in a time-dependent manner.

(0.42 ± 0.13, n = 13 versus 1.00 ± 0.21, n = 15, respectively, $P < 0.05$, Fig. 6A) was detected by qPCR. A quantification of TGF-β expression by Western blotting of graft lysates was also performed and revealed a significant decrease in grafts from mice after administration of pirfenidone compared with grafts from mice on vehicle ($P < 0.05$, n = 3 for each column, Fig. 6B). A pronounced TGF-β staining on vehicle as compared to pirfenidone 6 days after transplantation was detected (Fig. 6C). A significantly decreased number of TGF-β–positive cells after treatment with pirfenidone as compared to vehicle ($P < 0.05$,

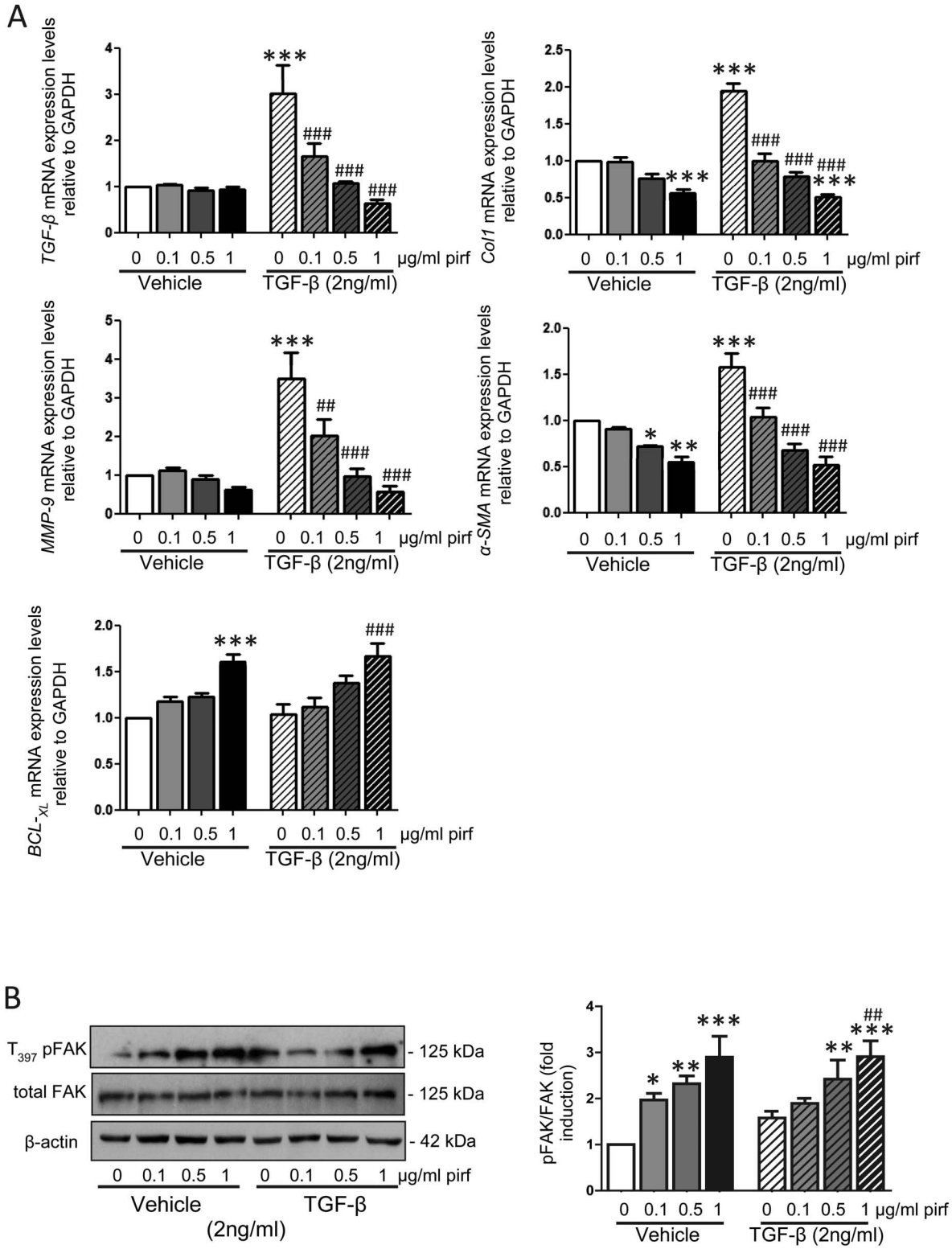

FIGURE 4. TGF-β1 mRNA is significantly decreased after administration of pirfenidone in intestinal fibroblasts in vitro. Increased pFAK after administration of pirfenidone compared to control. TGF-β, COL1A1, MMP-9, and α-SMA mRNA expressions are decreased, and BCL-$_{XL}$ mRNA expression is increased after treatment with pirfenidone compared to vehicle (*$P < 0.05$, **$P < 0.01$, ***$P < 0.001$, ##$P < 0.01$, ###$P < 0.001$, n= 5 each column, error bars = SEM, A). Western blotting (left) and densitometric analysis (right) showed significant increase in the ratio pFAK/total FAK after treatment with pirfenidone (*$P < 0.05$, **$P < 0.01$, ***$P < 0.001$, ##$P < 0.01$, n = 4, error bars = SEM, B).

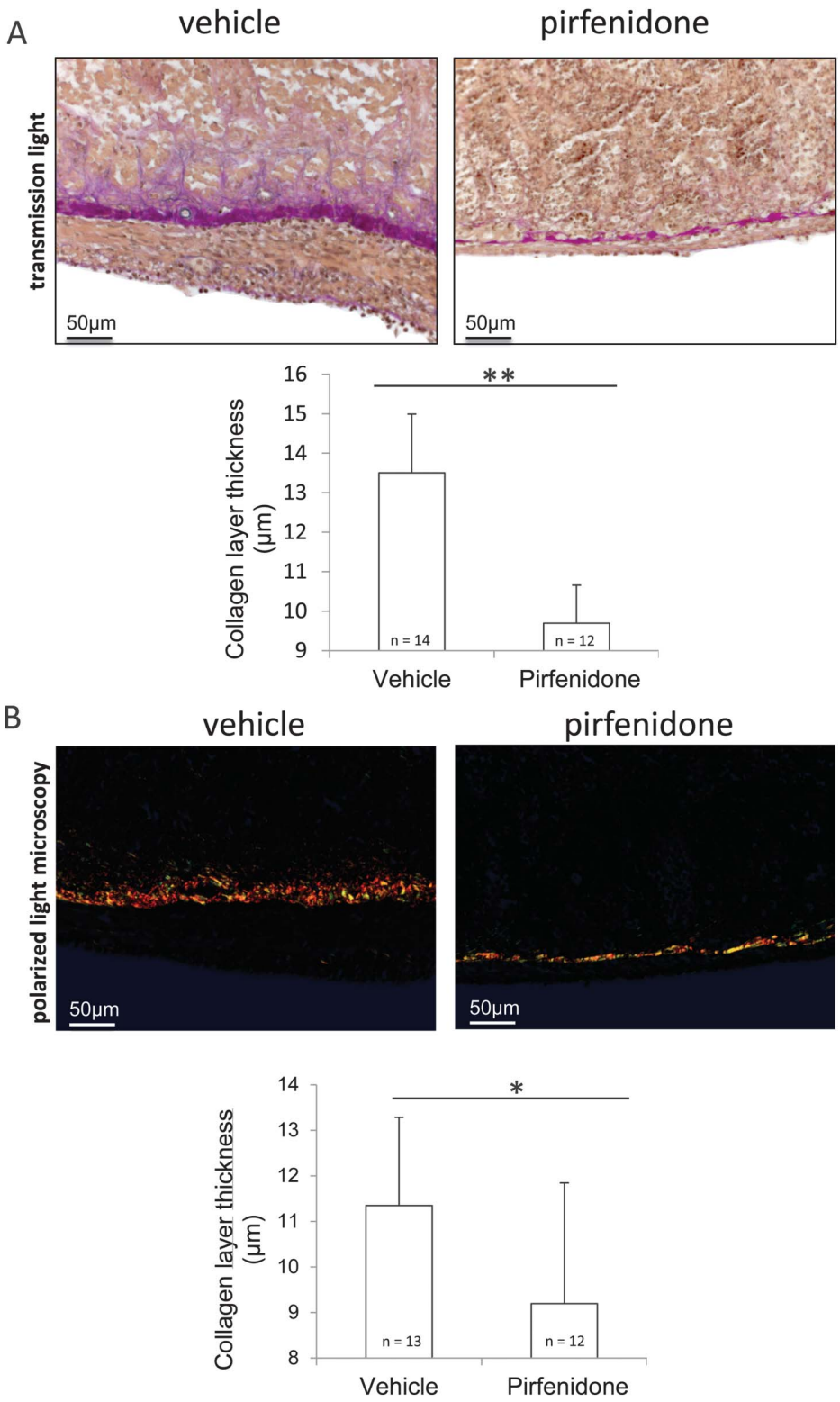

FIGURE 5. Collagen layer thickness is significantly decreased after administration of pirfenidone in grafts from the heterotopic transplantation model. Sirius red staining. (A) Transmission light showed significantly decreased collagen layer thickness after treatment with pirfenidone compared to vehicle (**$P < 0.001$). (B) Polarizing light microscopy confirmed significantly decreased collagen layer thickness after treatment with pirfenidone (*$P < 0.05$), n = 12 to 14 as indicated. Thickness was calculated from at least 8 places in representative areas at 10-fold magnification for each single graft. Mean value and SD are shown.

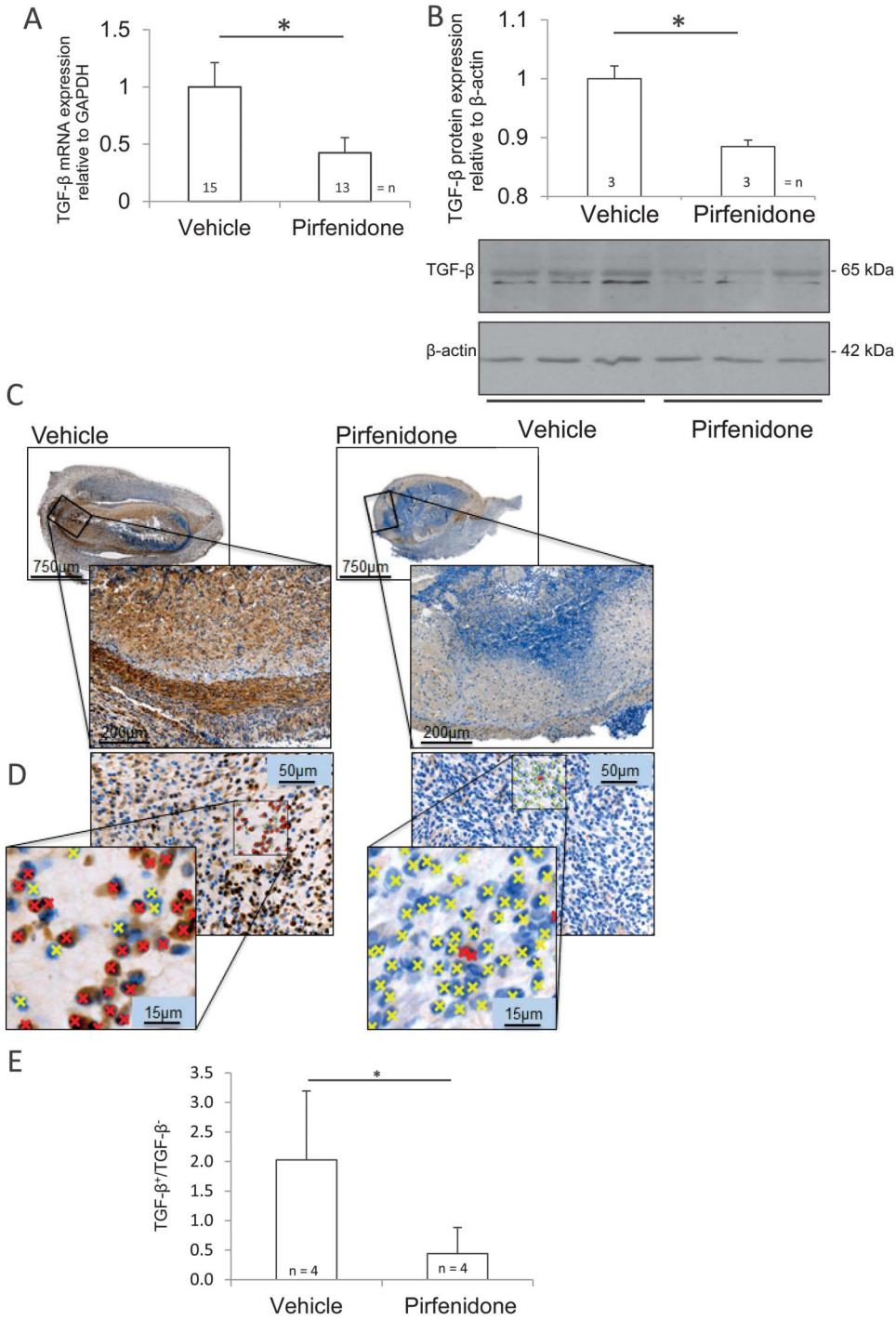

FIGURE 6. TGF-β1 is significantly decreased after administration of pirfenidone in grafts from the heterotopic transplantation model. (A) Significant decrease in TGF-β mRNA expression after treatment with pirfenidone compared to vehicle (*$P < 0.05$, n = 13 and 15, respectively). (B) Western blotting confirmed significant decrease in TGF-β after administration of pirfenidone (*$P < 0.05$, n = 3 for each column). Error bars = SD. Grafts exhibited a pronounced TGF-β staining (3,3′-diaminobenzidine, brown) on vehicle compared with pirfenidone. (C) Immunohistochemistry reveals a significant decrease in TGF-β1–positive cells after treatment with pirfenidone. (D and E) Number of TGF-β–positive cells (red crosses) was significantly increased on vehicle (*$P < 0.05$, Kruskal–Wallis one-way analysis of variance on ranks, all-pairwise multiple comparison procedures (Holm–Sidak method), D and E). Number of TGF-β–positive cells was normalized to the number of total cells (nuclei labeled by yellow and red crosses).

Fig. 6D, E) confirmed the qPCR and Western blot data. TGF-β was therefore shown to be decreased in the heterotopic intestinal grafts after administration of pirfenidone.

pFAK Is Significantly Increased in Grafts After Treatment with Pirfenidone

Western blotting revealed increased phosphorylation of FAK after administration of pirfenidone (Fig. 7A, n = 4 each group). A quantification of FAK phosphorylation was also performed and revealed significantly increased pFAK after treatment with pirfenidone ($P < 0.01$). Western blotting also revealed unchanged expression of total FAK after administration of pirfenidone. In line with in vitro experiments, α-SMA mRNA expression was significantly decreased (n = 9 each column, $P < 0.05$, Fig. 7B), and prosurvival BCL-$_{XL}$ mRNA expression was significantly increased after treatment with pirfenidone (n = 9 each column, $P < 0.05$, Fig. 7B).

Matrix Degrading MMPs and Proinflammatory Cytokines Are Decreased After Administration of Pirfenidone

We determined the expression of tissue remodeling proteases MMP-2, MMP-9, MMP-13, and the TIMP-1 in intestinal transplants by real-time PCR. Grafts from mice treated with pirfenidone showed a significant decrease in MMP-9 mRNA expression compared with vehicle (0.46 ± 0.24 versus 1.00 ± 0.62 mRNA expression level relative to GAPDH, $P < 0.05$, Fig. 8A). Similar, MMP-2, MMP-13, and TIMP-1 mRNA expressions were decreased after treatment with pirfenidone compared with vehicle (0.59 ± 0.50 versus 1.00 ± 0.68, 0.60 ± 0.72 versus 1.00 ± 1.01, and 0.42 ± 0.43 versus 1.00 ± 0.92 mRNA expression level relative to GAPDH, respectively, not significant, Fig. 8A). Transplants from mice treated with pirfenidone also showed a decrease in mRNA of proinflammatory cytokines IL-1β, IL-6, and MCP-1 as compared to vehicle (0.42 ± 0.43 versus 1.00 ± 0.92, 0.52 ± 0.38 versus 1.00 ± 0.89, and 0.53 ± 0.44 versus 1.00 ± 0.88 mRNA expression level relative to GAPDH, respectively, not significant, Fig. 8B). LOXL-2 is a copper-dependent matrix amine oxidase and a member of the lysyl oxidase enzyme family. The function of this oxidase is the stabilization of collagen fibrils and fibers in the extracellular matrix. Grafts from mice treated with pirfenidone showed a decrease in mRNA of LOXL-2 and also the major component of type I collagen COL1A1 and COL3A1, frequently found in association with type I collagen compared to vehicle (0.54 ± 0.431 versus 1.00 ± 0.67, 0.71 ± 0.65 versus 1.00 ± 0.87, and 0.57 ± 0.59 versus 1.00 ± 0.96 mRNA expression level relative to GAPDH, respectively, not significant, Fig. 8C).

DISCUSSION

In this study, we describe a new murine model of intestinal fibrosis. Heterotopic transplantation of small bowel resections in mice was followed by a rapid and constant fibrosis of the intestinal wall. The method is based on a recently described rat model of fibrosis as a substantial advance in understanding the formation of intestinal fibrosis.[16] Small bowel resections of donor mice were implanted into subcutaneous pouches of recipients. Grafts showed complete fibrosis in a time-dependent manner characterized by an increased deposition of collagen. EvG and sirius red staining confirmed significantly increased collagen layer thickness in transplants and revealed a diffuse network of fibrils in

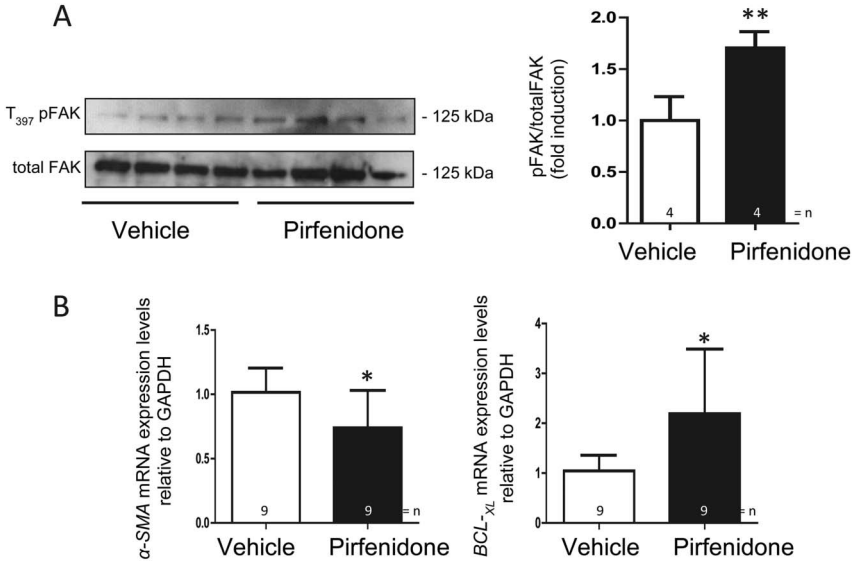

FIGURE 7. Increased pFAK after administration of pirfenidone compared to control in grafts from the heterotopic transplantation model. (A) Western blotting (left) and densitometric analysis (right) showed significant increase in the ratio pFAK/total FAK after treatment with pirfenidone (**$P < 0.01$, n = 4 for each column, error bars = SEM). (B) α-SMA mRNA expression is significantly decreased, whereas BCL-$_{XL}$ mRNA expression is significantly increased after treatment with pirfenidone compared to vehicle (*$P < 0.05$, n = 9 each column, error bars = SEM).

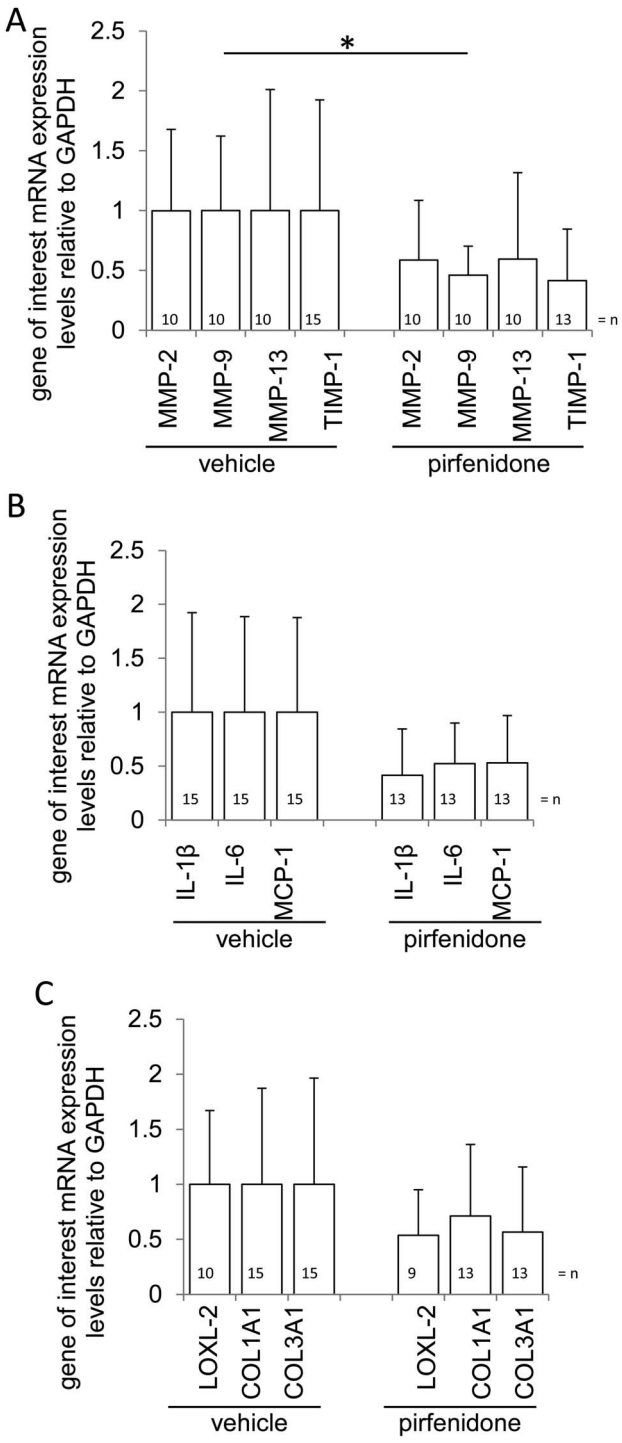

FIGURE 8. MMPs and proinflammatory cytokines are decreased after administration of pirfenidone in grafts from the heterotopic transplantation model. MMP-2, MMP-9, MMP-13, and TIMP-1 are decreased after treatment with pirfenidone compared to vehicle (*$P < 0.05$, Kruskal–Wallis one-way analysis of variance on ranks, all-pairwise multiple comparison procedures (Holm–Sidak method), A). IL-1β, IL-6, and MCP-1 are decreased after treatment with pirfenidone (B). LOXL-2, COL1A1, and COL3A1 are decreased after treatment with pirfenidone (C). N = 13 to 15 for each column, error bars = SD.

the obliterated lumen. In addition, immunohistochemistry revealed a time-dependent increase of TGF-β.

Fibrosis is traditionally viewed as the endpoint of a long-term process consisting of a chronic response of the digestive tract. Accordingly, intestinal fibrosis is viewed as a slow, unidirectional process,[27] in which inflammation encourages local fibroblast to multiply and deposit extracellular matrix as part of a wound-healing process. Although not necessarily incorrect, based on our results, this view should be extended to the observation that fibrosis could also be rapidly initiated and increased. Recent studies also suggest fibrogenesis as a very early process associated with inflammation.[28] Results from our own studies support this hypothesis as rapid increase of collagen layer thickness, fast development of occlusion, and rapid increase of TGF-β in grafts can be determined shortly after transplantation.

The antifibrotic effect of pirfenidone was successfully tested both in vitro and in our new model of intestinal fibrosis. In *in vitro* experiments, we determined a significant decrease in TGF-β, COL1A1, MMP-9, and α-SMA mRNA expressions after administration of pirfenidone in a dose-dependent manner compared with vehicle. This shows that hallmarks of progressive development of fibrosis are decreased after treatment with pirfenidone in intestinal fibroblasts.

Studies concerning fibroblasts of other tissues revealed that pFAK is a central regulator of cell migration in health and disease.[29–32] FAK is a nonreceptor protein tyrosine kinase involved in integrin-mediated control of cell behavior. The amount of FAK protein phosphorylation is increased during cell migration.[33] The autophosphorylation of FAK at the tyrosine residue 397 is a marker for the activation of FAK. Phosphorylation creates an SH2 binding site for different signaling and adapter proteins.[32,34] Migration of colonic fibroblasts is stimulated by growth factors like TGF-β, platelet-derived growth factor (PDGF)-AB, insulin-like growth factor (IGF)-I, and epidermal growth factor. Colonic fibroblasts also stimulate their own migration through an autocrine mechanism.[26] Migratory potential of colonic fibroblasts from patients with IBD is reduced compared with normal colonic fibroblasts, which is correlated with diminished FAK phosphorylation.[35] In contrast to TGF-β, FAK protein phosphorylation and BCL-$_{XL}$ mRNA expression are increased after administration of pirfenidone in our studies. This suggests an increased migratory potential and viability of cells and is confirmative with results from the performed wounding assay that revealed an advanced wound closure after treatment with pirfenidone. In our murine model of intestinal fibrosis, we determined a significantly deceased collagen layer thickness in harvested grafts from mice after administration of oral pirfenidone in comparison to vehicle-treated mice. Furthermore, TGF-β expression on mRNA and protein level was significantly reduced by pirfenidone. Confirmative to the in vitro experiments, FAK protein phosphorylation and BCL-$_{XL}$ mRNA expressions were increased after treatment with pirfenidone suggesting an increased migratory potential and viability of cells in the graft. Grafts from mice treated with pirfenidone showed

a significant decrease in α-SMA and MMP-9 mRNA expression compared to vehicle. MMP-2, MMP-13, TIMP-1, IL-1β, IL-6, MCP-1, and LOXL-2 mRNA expressions also were reduced.

Pirfenidone is known to exhibit antifibrotic and anti-inflammatory effects in a variety of organs by modulating various genes known to be involved in wound healing and fibrosis, including TGF-β, MMP-2, and MMP-9.[19,20,23,24,36] Graham and Diegelmann[37] showed that TGF-β promotes collagen deposition by smooth muscle cells isolated from CD tissue, a process that may play a significant role in stricture formation and fibrosis in patients with CD. In addition, TGF-β is known to inhibit intestinal epithelial cell proliferation, a process that may inhibit re-epithelialization after surface injury.[38–40] The gelatinases (MMP-2 and MMP-9) degrade denatured collagen of all types.[41] MMP-2 and MMP-9 are upregulated in patients with IBD in active flares.[42–45] MMP-2 is expressed in almost all tissues and is markedly increased in IBD tissues.[46] MMP-9 activity and protein expression are upregulated during dextran sulphate sodium colitis, and in normal colonic mucosa, the expression is absent.[47] MMP-9$^{-/-}$ mice have significantly less severe DSS-induced colitis with reduced inflammation and mucosal injury.[48]

Thus, pirfenidone may be a new treatment option to prevent fibrogenesis and development of strictures in patients with IBD. In patients with IPF after 72 weeks following daily pirfenidone administration, following adverse effects could be detected with an increased incidence: nausea, rash, dyspepsia, dizziness, vomiting, photosensitivity reaction, anorexia, arthralgia, insomnia, abdominal distention, decreased appetite, stomach discomfort, weight reduction, abdominal pain, asthenia, pharyngolaryngeal pain, pruritus, and hot flush.[17]

The described heterotopic transplantation in mice will serve as a new model to develop treatments targeted at intestinal fibrosis and provide the opportunity of using genetically altered animals. Important aspects of human intestinal fibrosis are reflected in our model of heterotopic transplantation in mice. It may also be instrumental in deciphering the formation of intestinal fibrosis at the molecular level. The utilization of our new in vivo heterotopic transplant animal model of intestinal fibrosis may ultimately lead to novel interventions in the prevention of treatment of intestinal fibrosis. We were able to confirm the postulated antifibrotic effects of pirfenidone. Thus, pirfenidone may be a new treatment option to prevent intestinal fibrosis formation in IBD.

ACKNOWLEDGMENTS

The authors thank PD Dr. med. Christian Clarenbach (Department of Pulmonology, University Hospital Zurich, Switzerland), Patrick Kolb (Country Coordinator Switzerland, InterMune Schweiz GmbH), and Hisashi Oku, PhD (Shionogi & Co., Ltd) for helpful discussions with Pirfenidone application. The authors thank André Fitsche (Institute of Surgical Pathology, University Hospital Zurich, Zurich, Switzerland) for his support with immunohistochemical stainings.

Author contributions: study concept: G. Rogler, acquisition of data: R. Meier, C. Lutz, S. Fagagnini, G. Bollmann, A. Hünerwadel, J. Cosin-Roger, and M. Hausmann, critical revision of the manuscript: G. Rogler, F. E. Weber, M. Hausmann, and A. Weber, and technical support: C. Mamie, S. Lang, and A. Tchouboukov.

REFERENCES

1. Jones MK, Tomikawa M, Mohajer B, et al. Gastrointestinal mucosal regeneration: role of growth factors. *Front Biosci.* 1999;4:D303–D309.
2. Rieder F, Brenmoehl J, Leeb S, et al. Wound healing and fibrosis in intestinal disease. *Gut*. 2007;56:130–139.
3. Sartor RB. Current concepts of the etiology and pathogenesis of ulcerative colitis and Crohn's disease. *Gastroenterol Clin North Am.* 1995; 24:475–507.
4. Pardo A, Selman M. Matrix metalloproteases in aberrant fibrotic tissue remodeling. *Proc Am Thorac Soc.* 2006;3:383–388.
5. Kim H, Oda T, Lopez-Guisa J, et al. TIMP-1 deficiency does not attenuate interstitial fibrosis in obstructive nephropathy. *J Am Soc Nephrol.* 2001; 12:736–748.
6. Underwood DC, Osborn RR, Bochnowicz S, et al. SB 239063, a p38 MAPK inhibitor, reduces neutrophilia, inflammatory cytokines, MMP-9, and fibrosis in lung. *Am J Physiol Lung Cell Mol Physiol.* 2000;279: L895–L902.
7. Vaillant B, Chiaramonte MG, Cheever AW, et al. Regulation of hepatic fibrosis and extracellular matrix genes by the th response: new insight into the role of tissue inhibitors of matrix metalloproteinases. *J Immunol.* 2001; 167:7017–7026.
8. Bucala R, Spiegel LA, Chesney J, et al. Circulating fibrocytes define a new leukocyte subpopulation that mediates tissue repair. *Mol Med.* 1994;1:71–81.
9. Cosnes J, Cattan S, Blain A, et al. Long-term evolution of disease behavior of Crohn's disease. *Inflamm Bowel Dis.* 2002;8:244–250.
10. Freeman HJ. Natural history and clinical behavior of Crohn's disease extending beyond two decades. *J Clin Gastroenterol.* 2003;37:216–219.
11. D'Haens G, Geboes K, Rutgeerts P. Endoscopic and histologic healing of Crohn's (ileo-) colitis with azathioprine. *Gastrointest Endosc.* 1999;50: 667–671.
12. Vermeire S, van Assche G, Rutgeerts P. Review article: altering the natural history of Crohn's disease–evidence for and against current therapies. *Aliment Pharmacol Ther.* 2007;25:3–12.
13. Cosnes J, Nion-Larmurier I, Beaugerie L, et al. Impact of the increasing use of immunosuppressants in Crohn's disease on the need for intestinal surgery. *Gut*. 2005;54:237–241.
14. Johnson LA, Luke A, Sauder K, et al. Intestinal fibrosis is reduced by early elimination of inflammation in a mouse model of IBD: impact of a "Top-Down" approach to intestinal fibrosis in mice. *Inflamm Bowel Dis.* 2012;18:460–471.
15. Boehler A, Chamberlain D, Kesten S, et al. Lymphocytic airway infiltration as a precursor to fibrous obliteration in a rat model of bronchiolitis obliterans. *Transplantation*. 1997;64:311–317.
16. Hausmann M, Rechsteiner T, Caj M, et al. A new heterotopic transplant animal model of intestinal fibrosis. *Inflamm Bowel Dis.* 2013;19:2302–2314.
17. Noble PW, Albera C, Bradford WZ, et al. Pirfenidone in patients with idiopathic pulmonary fibrosis (CAPACITY): two randomised trials. *Lancet*. 2011;377:1760–1769.
18. Al-Bayati MA, Xie Y, Mohr FC, et al. Effect of pirfenidone against vanadate-induced kidney fibrosis in rats. *Biochem Pharmacol.* 2002;64: 517–525.
19. Lee KW, Everett THt, Rahmutula D, et al. Pirfenidone prevents the development of a vulnerable substrate for atrial fibrillation in a canine model of heart failure. *Circulation*. 2006;114:1703–1712.
20. Di Sario A, Bendia E, Macarri G, et al. The anti-fibrotic effect of pirfenidone in rat liver fibrosis is mediated by downregulation of procollagen alpha1(I), TIMP-1 and MMP-2. *Dig Liver dis.* 2004;36:744–751.
21. Armendariz-Borunda J, Lyra-Gonzalez I, Medina-Preciado D, et al. A controlled clinical trial with pirfenidone in the treatment of pathological skin scarring caused by burns in pediatric patients. *Ann Plast Surg.* 2012; 68:22–28.
22. Schaefer CJ, Ruhrmund DW, Pan L, et al. Antifibrotic activities of pirfenidone in animal models. *Eur Respir Rev.* 2011;20:85–97.

23. Oku H, Shimizu T, Kawabata T, et al. Antifibrotic action of pirfenidone and prednisolone: different effects on pulmonary cytokines and growth factors in bleomycin-induced murine pulmonary fibrosis. *Eur J Pharmacol.* 2008;590:400–408.
24. Lee BS, Margolin SB, Nowak RA. Pirfenidone: a novel pharmacological agent that inhibits leiomyoma cell proliferation and collagen production. *J Clin Endocrinol Metab.* 1998;83:219–223.
25. Spagnolo P, Del Giovane C, Luppi F, et al. Non-steroid agents for idiopathic pulmonary fibrosis. *Cochrane Database Syst Rev.* 2010;9:CD003134.
26. Leeb SN, Vogl D, Falk W, et al. Regulation of migration of human colonic myofibroblasts. *Growth Factors.* 2002;20:81–91.
27. Pinzani M. Fibrosis in the GI tract: pathophysiology, diagnosis and treatment options. *Front Gastrointest Res.* 2010;26:15–31.
28. Rieder F, Kessler S, Sans M, et al. Animal models of intestinal fibrosis: new tools for the understanding of pathogenesis and therapy of human disease. *Am J Physiol Gastrointest Liver Physiol.* 2012;303:G786–G801.
29. Abedi H, Zachary I. Signalling mechanisms in the regulation of vascular cell migration. *Cardiovasc Res.* 1995;30:544–556.
30. Brunton VG, Ozanne BW, Paraskeva C, et al. A role for epidermal growth factor receptor, c-Src and focal adhesion kinase in an in vitro model for the progression of colon cancer. *Oncogene.* 1997;14:283–293.
31. Haq F, Trinkaus-Randall V. Injury of stromal fibroblasts induces phosphorylation of focal adhesion proteins. *Curr Eye Res.* 1998;17:512–523.
32. Schlaepfer DD, Hauck CR, Sieg DJ. Signaling through focal adhesion kinase. *Prog Biophys Mol Biol.* 1999;71:435–478.
33. Liu YW, Sanders MA, Basson MD. Human Caco-2 intestinal epithelial motility is associated with tyrosine kinase and cytoskeletal focal adhesion kinase signals. *J Surg Res.* 1998;77:112–118.
34. Sieg DJ, Hauck CR, Schlaepfer DD. Required role of focal adhesion kinase (FAK) for integrin-stimulated cell migration. *J Cell Sci.* 1999; 112 (pt 16):2677–2691.
35. Leeb SN, Vogl D, Gunckel M, et al. Reduced migration of fibroblasts in inflammatory bowel disease: role of inflammatory mediators and focal adhesion kinase. *Gastroenterology*. 2003;125:1341–1354.
36. Wynn TA. Cellular and molecular mechanisms of fibrosis. *J Pathol.* 2008; 214:199–210.
37. Graham MFBG, Diegelmann RF. Transforming growth factor beta 1 selectively augments collagen synthesis by human intestinal smooth muscle cells. *Gastroenterology*. 1990;99:447–453.
38. Barnard JA, Beauchamp RD, Coffey RJ, et al. Regulation of intestinal epithelial cell growth by transforming growth factor type beta. *Proc Natl Acad Sci U S A.* 1989;86:1578–1582.
39. Koyama SY, Podolsky DK. Differential expression of transforming growth factors alpha and beta in rat intestinal epithelial cells. *J Clin Invest.* 1989;83:1768–1773.
40. Suemori S, Ciacci C, Podolsky DK. Regulation of transforming growth factor expression in rat intestinal epithelial cell lines. *J Clin Invest.* 1991; 87:2216–2221.
41. Allan JA, Docherty AJ, Barker PJ, et al. Binding of gelatinases A and B to type-I collagen and other matrix components. *Biochem J.* 1995;309 (pt 1): 299–306.
42. von Lampe B, Barthel B, Coupland SE, et al. Differential expression of matrix metalloproteinases and their tissue inhibitors in colon mucosa of patients with inflammatory bowel disease. *Gut.* 2000;47:63–73.
43. Bailey CJ, Hembry RM, Alexander A, et al. Distribution of the matrix metalloproteinases stromelysin, gelatinases A and B, and collagenase in Crohn's disease and normal intestine. *J Clin Pathol.* 1994;47:113–116.
44. Baugh MD, Perry MJ, Hollander AP, et al. Matrix metalloproteinase levels are elevated in inflammatory bowel disease. *Gastroenterology*. 1999;117:814–822.
45. Baugh MD, Evans GS, Hollander AP, et al. Expression of matrix metalloproteases in inflammatory bowel disease. *Ann N Y Acad Sci.* 1998;859: 249–253.
46. Gao Q, Meijer MJ, Kubben FJ, et al. Expression of matrix metalloproteinases-2 and -9 in intestinal tissue of patients with inflammatory bowel diseases. *Dig Liver Dis.* 2005;37:584–592.
47. Castaneda FE, Walia B, Vijay-Kumar M, et al. Targeted deletion of metalloproteinase 9 attenuates experimental colitis in mice: central role of epithelial-derived MMP. *Gastroenterology*. 2005;129:1991–2008.
48. Santana A, Medina C, Paz-Cabrera MC, et al. Attenuation of dextran sodium sulphate induced colitis in matrix metalloproteinase-9 deficient mice. *World J gastroenterol.* 2006;12:6464–6472.